Heliyon 10 (2024) e26294

Contents lists available at ScienceDirect

Heliyon

journal homepage: www.cell.com/heliyon

Research article

# Hybrid cortical bone trajectory and modified cortical bone trajectory techniques in transforaminal lumbar interbody fusion at L4-L5 segment: A finite element analysis

Yixi Wang [a,b,1], Abulikemu Maimaiti [b,1], Yang Xiao [b], Abudusalamu Tuoheti [b], Rui Zhang [b], Muzaipaer Maitusong [a], Qihao Chen [b], Paerhati Rexiti [b,c,d,*]

[a] *First Clinical Medical College, Xinjiang Medical University, Urumqi, China*
[b] *Department of Spine Surgery, The First Affiliated Hospital of Xinjiang Medical University, Urumqi, China*
[c] *Key Laboratory of High Incidence Disease Research in Xinjiang (Xinjiang Medical University), Ministry of Education, Urumqi, China*
[d] *Xinjiang Clinical Research Center for Orthopedics, Urumqi, China*

ARTICLE INFO

*Keywords:*
Finite element analysis
Hybrid fixation
Modified cortical bone trajectory
Cortical bone trajectory
Transforaminal lumbar interbody fusion

ABSTRACT

*Background:* The academia has increasingly acknowledged the superior biomechanical performance of the hybrid fixation technique in recent years. However, there is a lack of research on the hybrid fixation technique using BCS (Bilateral Cortical Screws) and BMCS (Bilateral Modified Cortical Screws). This study aims to investigate the biomechanical performance of the BCS and BMCS hybrid fixation technique in transforaminal lumbar interbody fusion (TLIF) at the L4-L5 segment in a complete lumbar-sacral finite element model.

*Methods:* Three cadaver specimens are used to construct three lumbar-sacral finite element models. The biomechanical properties of various fixation technologies (BCS-BCS, BMCS-BMCS, BMCS-BCS, and BCS-BMCS) are evaluated at the L4-5 segment with a TLIF procedure conducted, including the range of motion (ROM) of the L4-5 segment, as well as the stress experienced by the cage, screws, and rods. The testing is conducted under specific loading conditions, including a compressive load of 400 N and a torque of 7.5Nm, subjecting the model to simulate flexion, extension, lateral bending, and rotation.

*Results:* No significant variations are seen in the ROM at the L4-5 segment when comparing the four fixation procedures during flexion and extension. However, when it comes to lateral bending and rotation, the ROM is ordered in descending order as BCS-BCS, BCS-BMCS, BMCS-BMCS, and BMCS-BCS. The maximum stress experienced by the cage is observed to be highest within the BMCS-BCS technique during movements including flexion, extension, and lateral bending. Conversely, the BMCS-BMCS technique exhibits the highest cage stress levels during rotational movements. The stress applies to the screws and rods order the sequence of BCS-BCS, BCS-BMCS, BMCS-BCS, and BMCS-BMCS throughout all four working conditions.

*Conclusion:* The BMCS-BCS technique shows better biomechanical performance with less ROM and lower stress on the internal fixation system compared to other fixation techniques. BMCS-BMCS technology has similar mechanical performance to BMCS-BCS but has more contact area between screws and cortical bone, making it better for patients with severe osteoporosis.

* Corresponding author. Department of Spine Surgery, The First Affiliated Hospital of Xinjiang Medical University, Urumqi, Xinjiang Uygur Autonomous Region, 830054, China.

*E-mail address:* parhart@vip.sina.com (P. Rexiti).

[1] These authors have contributed equally.

https://doi.org/10.1016/j.heliyon.2024.e26294
Received 23 August 2023; Received in revised form 3 February 2024; Accepted 9 February 2024
Available online 20 February 2024

**Abbreviations**

| | |
|---|---|
| TLIF | Transforaminal lumbar interbody fusion |
| PLIF | Posterior lumbar interbody fusion |
| TT | Traditional trajectory |
| CBT | Cortical bone trajectory |
| MCBT | Modified cortical bone trajectory |
| PS | Pedicle screw |
| BCS | Bilateral cortical bone trajectory screw |
| BMCS | Bilateral modified cortical bone trajectory screw |
| FE | Finite element |
| ROM | Range of motion |
| ALL | Anterior longitudinal ligament |
| PLL | Posterior longitudinal ligament |
| ITL | Intertransverse ligament |
| LF | Ligamentum flavum |
| CL | Capsular ligament |
| ISL | Interspinous ligament |
| SSL | Supraspinous ligament |
| BMD | Bone mineral density |
| CT | Computerized tomography |
| VAS | Visual Analog Scale |
| ODI | Oswestry Disability Index |
| DICOM | Digital Imaging and Communications in Medicine |
| ASD | Adjacent segment disease |
| TET | Tetrahedral |

## 1. Introduction

Professor Santoni has presented a novel viable internal fixation method, referred to as the cortical bone trajectory (CBT), to effectively tackle the problem of pedicle screws (PS) loosening in persons diagnosed with osteoporosis [1]. Compared with the traditional trajectory (TT), CBT entails a downward and inward shift of the screw entrance point, which contributes to an augmentation of both the lateral and cephalic angles of the screw trajectory. Consequently, there is a notable augmentation in the contact surface area between the CBT screw and the cortical bone, thereby improving CBT fixation's effectiveness in persons with osteoporosis [2]. In addition, the utilization of CBT has some minimally invasive benefits, including reduced incision size, shorter duration of surgery, and less blood loss compared to TT, which can positively impact the postoperative recuperation of patients [3].

The surgical procedure referred to as Posterior Lumbar Interbody Fusion (PLIF) was first introduced by Cloward and has since been widely embraced and employed in medical practice [4]. However, this approach requires excessive traction on the nerve roots and dura mater during the surgical intervention in order to generate sufficient surgical area, thereby increasing the probability of nerve injury [5,6]. To address this potential risk, Harms et al. developed the Transforaminal Lumbar Interbody Fusion (TLIF) technique, which involves performing disc removal, bone grafting, and implantation of a fusion device through a unilateral intervertebral foramen [7]. In contrast to the PLIF technique, the TLIF technique provides a broader surgical area while reducing the potential for excessive tension on the nerve roots and dura mater [8]. Furthermore, the TLIF procedure could preserve the more spinous process and ligaments, reducing the surgical area and maintaining an elevated level of spinal stability after the surgical intervention [9].

Previous studies have demonstrated that, during a five-year follow-up period, the patients accept CBT screw with TLIF technique yield superior Visual Analog Scale (VAS) and Oswestry Disability Index (ODI) scores compared to the patients receiving PS in conjunction with TLIF technology [10]. Nevertheless, it is essential to acknowledge that the CBT technique possesses certain limitations, including a shorter screw trajectory length, unstable mechanical performance, and the potential for damaging intervertebral discs, which may all impact the procedure's efficacy and have adverse consequences [11,12]. To deal with the above problems, the Modified Cortical bone trajectory (MCBT) technique has been proposed, which involves more inward movement of the screw entry point, further increasing the screw trajectory's lateral angle and reducing the cephalic angle, which aims to enhance the contact area between the screw and the thicker inferior and medial cortical bone of the pedicle [13]. Preliminary research has indicated that the MCBT technique exhibits superior biomechanical properties compared to both CBT and TT techniques in scenarios involving lateral bending and axial rotation, and it is a viable option for individuals diagnosed with severe osteoporosis [14–16]. Nevertheless, subsequent investigations have brought to light certain limitations associated with the MCBT technique, including limited decompression of the lateral recess and intervertebral foramen, potential for screw insertion point splitting, and the risk of damaging the dura mater [17].

In prior studies, our team put forth the integration of MCBT and TT fixation methodologies for spine fixation and evaluated the biomechanical property of this approach by employing finite element models of both two-segment and complete lumbar-sacral vertebrae [17,18]. The experimental findings indicate that the utilization of the combined MCBT and TT techniques effectively compensates for the limitations associated with single fixation methods and showcases enhanced biomechanical performance [17,18]. Based on the aforementioned findings, we have subsequently developed a hybrid fixation technique that integrates CBT and MCBT technologies. The goal of this study is to compare the biomechanical performance of four different fixation techniques in a full lumbar spine model using finite element analysis, laying the groundwork for the clinical application of CBT and MCBT hybrid fixation techniques. The four fixation techniques are Bilateral Cortical Screw-Bilateral Cortical Screw (BCS-BCS), Bilateral Modified Cortical Screw-Bilateral Modified Cortical Screw (BMCS-BMCS), Bilateral Modified Cortical Screw-Bilateral Cortical Screw (BMCS-BCS), and Bilateral Cortical Screw-Bilateral Modified Cortical Screw (BCS-BMCS).

## 2. Materials and methods

### 2.1. Development of an intact L1-S1 finite element model

#### 2.1.1. Subjects

Three cadaver specimens are obtained from Xinjiang Medical University's School of Basic Medical Sciences. The subjects of the cadaver specimens ranged in age from 65 to 77 years old, with a mean age of 73 years. Table 1 presents some basic characteristic data of the three corpse specimens, which are recorded during their last medical service (Except T-score). A bone density test and computed tomography (CT) scan are performed on the three specimens, and the results show that the osteoporosis is primary (Bone density $T<-2.5$ SD) rather than secondary. The CT scanning procedure also effectively eliminates other possible medical confounding factors, including a history of lumbar spine surgery, infectious diseases, or microscopic bone tumor lesions.

#### 2.1.2. Surfaces

High-resolution CT scans of the L1-S1 vertebral bodies are undertaken for each subject using Brilliance equipment (PHILIPS, Netherlands), and the essential image data obtained from the CT scans are saved in the DICOM (Digital Imaging and Communications in Medicine) data file format. The DICOM data files are imported into the Mimics 17.0 software (Materialize, Belgium), delineation and specification of the anatomical orientations of the vertebrae, including anterior, posterior, superior, inferior, left, and right. After establishing anatomical directions, the positioning tool effectively detects and identifies grayscale images containing the vertebral body and its surrounding background. The grayscale images undergo a combination method of manual segmentation, threshold segmentation, and automatic adjustment techniques to complete the visualization of the L1-S1 vertebral regions. Subsequently, an artificial check is conducted at the level of each CT scan to eliminate any unacknowledged or redundant areas and mark the omitted areas. Following the acquisition of the initial 3D model, a process of smoothing and noise reduction is undertaken to improve the perceptibility of the contour boundaries of the whole model. After that, the self-extraction function and the erase fill feature in Mimics software are utilized to eliminate any lingering artifacts, holes, and noise observed in the improved model. Finally, the resulting three-dimensional skeletal models were stored in the STL file format.

#### 2.1.3. Meshing

The STL 3D files are subsequently subjected to a mesh adjustment procedure utilizing the 3-Matic software (Materialize, Belgium) in order to achieve optimal analysis. This process includes reconfiguring the grid geometry to reduce distortions during the model smoothing processes. Sandpaper tools are employed to finely refine and smooth the model structures, especially focusing on the posterior structures of the vertebral body, such as the facet joints and isthmus. The present study utilizes a hybrid meshing method that integrates two types of tetrahedral (TET) meshes (TET 4 and TET 10) in order to improve the accuracy of lumbar spine motion restoration. In the process of discretization, TET 10 meshes are applied to simulate the tissues with low stiffness, such as intervertebral discs, whereas TET 4 meshes are employed to simulate the highly rigid structures, such as vertebral bodies, spinous process, vertebral endplates, and so on. The mesh element size utilized for the L1-S1 spine vertebra model is 0.3 mm. In addition to the above steps, further optimization involves effectively refining the model's surface patches, thereby reducing the chance of morphological inaccuracies in the model. When each vertebra is optimized accordingly, the final construct of the L1-S1 vertebral model is achieved by optimizing the grille construction and employing a methodology of curved surface fitting.

#### 2.1.4. Material properties

The complete finite element model is composed of interconnected components including 5 lumbar vertebrae, 1 sacrum, and 5

**Table 1**
The specific parameters of the cadaver specimens.

| Parameters | Specimen 1 | Specimen 2 | Specimen 3 |
|---|---|---|---|
| Gender | Male | Male | Female |
| Age | 77 | 65 | 77 |
| Height (cm) | 171 | 178 | 166 |
| Weight (kg) | 51 | 81 | 42 |
| BMI | 17.4 | 25.6 | 15.2 |
| T Value (BMD) | −3.1 | −2.6 | −2.8 |
| Cause of death | Lung Cancer | Chronic Obstructive Pulmonary Disease | Gastric cancer |

intervertebral discs. Each segment of the model contained 2 endplates and 7 ligaments (Fig. 1 A, B). Regarding the cortical bone thickness, as presented in Fig. 1C, it lies between the range of 0.5–1 mm [19]. The cartilaginous structures attached to each vertebral endplate's upper and lower surfaces are assigned a thickness of 1 mm [20], as shown in Fig. 1 F. The nucleus pulposus, a major part of each intervertebral disc occupying 44% of the disc volume, is modeled as an incompressible fluid-filled cavity with low stiffness (Fig. 1 G) [21]. The facet joint cartilage is modeled with "soft frictionless contact," illustrated in Fig. 1 D, and is given an initial gap parameter of 0.5 mm [22]. Various ligaments, namely, the anterior longitudinal ligament (ALL), posterior longitudinal ligament (PLL), intertransverse ligament (ITL), ligamentum flavum (LF), capsular ligament (CL), interspinous ligament (ISL), and supraspinous ligament (SSL), are represented and subsequently assigned specific nonlinear material properties, as depicted in Fig. 1 E [17].

Finally, the assembled finite element meshed models are processed using the ANSYS Workbench 19.1 (ANSYS, Inc., Canonsburg, PA, USA). During this stage, material properties are set for each component of the model (Table 2) [23–26], ensuring that each represents its real-world counterpart as accurately as possible in terms of mechanical response and structural interactions.

### 2.1.5. Construction of surgical models

Before simulating screw insertion, it needs to mimic TLIF surgery in the L4-L5 segment in the finite element model, which needs to remove the decompression side facet joint. The L1-L5 finite element model is imported into MAYA 2019 (Autodesk Inc, USA), following the TLIF surgical principle, the facet joints and a section of the vertebral lamina in the L4-L5 segment needed to be removed are marked. After the completion of the design process, the model is transferred to 3-Matic software (Materialize, Belgium). Within 3-Matic, the Boolean calculation is used to perform a subtraction operation in the designated removed area within the L4-L5 segment. Given that the TLIF surgery involves the partial removal of facet joints on the decompression side, it follows that both the capsular ligament and the facet joint cartilage on the decompression side will be subtracted simultaneously during the Boolean operation within the finite element model.

The L4-L5 vertebral bodies are then fixed using the following screw combinations: (1) BCS-BCS group (CBT at the L4 and L5 segments, Fig. 2A); (2) BMCS-BMCS group (MCBT at the L4 and L5 segments, Fig. 2B); (3) BMCS-BCS group (MCBT at the L4, CBT at the L5, Fig. 2C); (4) BCS-BMCS group (CBT at the L4, MCBT at the L5, Fig. 2D). The CBT screws have a diameter of 5.0 mm and a length of 35 mm, while the MCBT screws have a diameter of 5.0 mm and a length of 40 mm. The entry point for the CBT screws is located on the outer side of the pars interarticularis, using a clock-face orientation. The screws are inserted on the left side pedicle at 5 o'clock and on the right side at 7 o'clock. The screw trajectory had a lateral angulation of 10° and a cephalic angulation of 25°. Compared to the CBT technique, the entry point for the MCBT screws is shifted inward by 2–3 mm, with an increased lateral angulation and decreased cephalic angulation. The exact location of the MCBT screw entrance point and the angle of the trajectory can be found in a previously published article [12].

## 2.2. Boundary and loading conditions

During the analysis, the sacrum is rigidly immobilized and restricted to prevent any displacement or rotation when a force is exerted on the L1 vertebral body. In order to replicate the weight and motion load exerted on the human body, a designated point of reference is formed at the central region of the upper surface of the L1 vertebral body. This reference point is then coupled to the upper

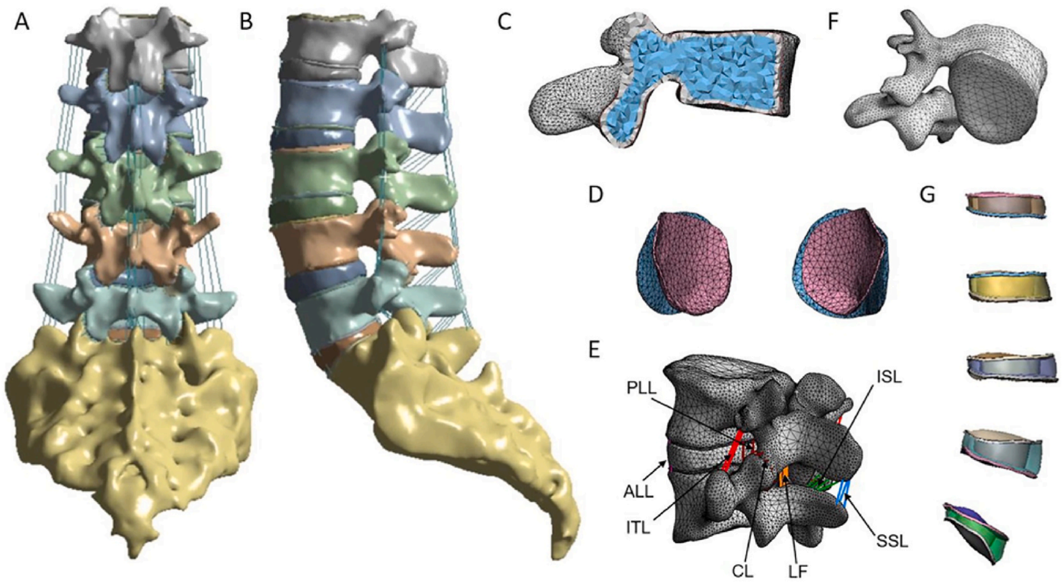


**Fig. 1.** Schematic diagram of L1-S1 finite element models [17]. A: Back view, B: Sagittal view, C: Regional thickness of the cortical bone, D: Facet cartilage, E: Ligaments, F: Vertebral endplate, G: Intervertebral discs.

**Table 2**
Material properties in the current study [23–26].

| Materials | Young's Modulus (Mpa) | Poisson's Ratio | Density (kg/mm3) | Cross-Sectional Area (mm2) | Radius ( mm ) |
|---|---|---|---|---|---|
| Cortical bone | 12,000 | 0.3 | 1.91 | – | – |
| Cancellous bone | 100 | 0.2 | 1.87 | – | – |
| Cartilaginous endplate | 23.8 | 0.4 | 1.0003 | – | – |
| Facet cartilage | 24 | 0.4 | – | – | – |
| Annulus fibrosis | 4.2 | 0.45 | – | – | – |
| Nucleus pulposus | 1 | 0.4999 | – | – | – |
| ALL | 7.8(<12.0%) 20.0(>12.0%) | – | 1.00e-06 | 63.7 | 4.5029 |
| PLL | 10.0(<11.0%) 20.0(>11.0%) | – | 1.00e −06 | 20 | 2.5231 |
| CL | 7.5(<25.0%) 32.9(>25.0%) | – | 1.00e −06 | 30 | 3.0902 |
| LF | 15.0(<6.2%) 19.5(>6.2%) | – | 1.00e-06 | 40 | 3.5682 |
| ISL | 10.0(<14.0%) 11.6(>14.0%) | – | 1.00e-06 | 40 | 3.5682 |
| SSL | 8.0(<20.0%) 15(>20.0%) | – | 1.00e-06 | 30 | 3.0902 |
| ITL | 10.0(<18.0%) 58.7(>18.0%) | – | 1.00e-06 | 1.8 | 0.7569 |
| Cage (PEEK) | 3600 | 0.25 | 1.32e−6 | – | – |
| Screw and Rod (Titanium) | 110,000 | 0.3 | 4.5e−6 | – | – |

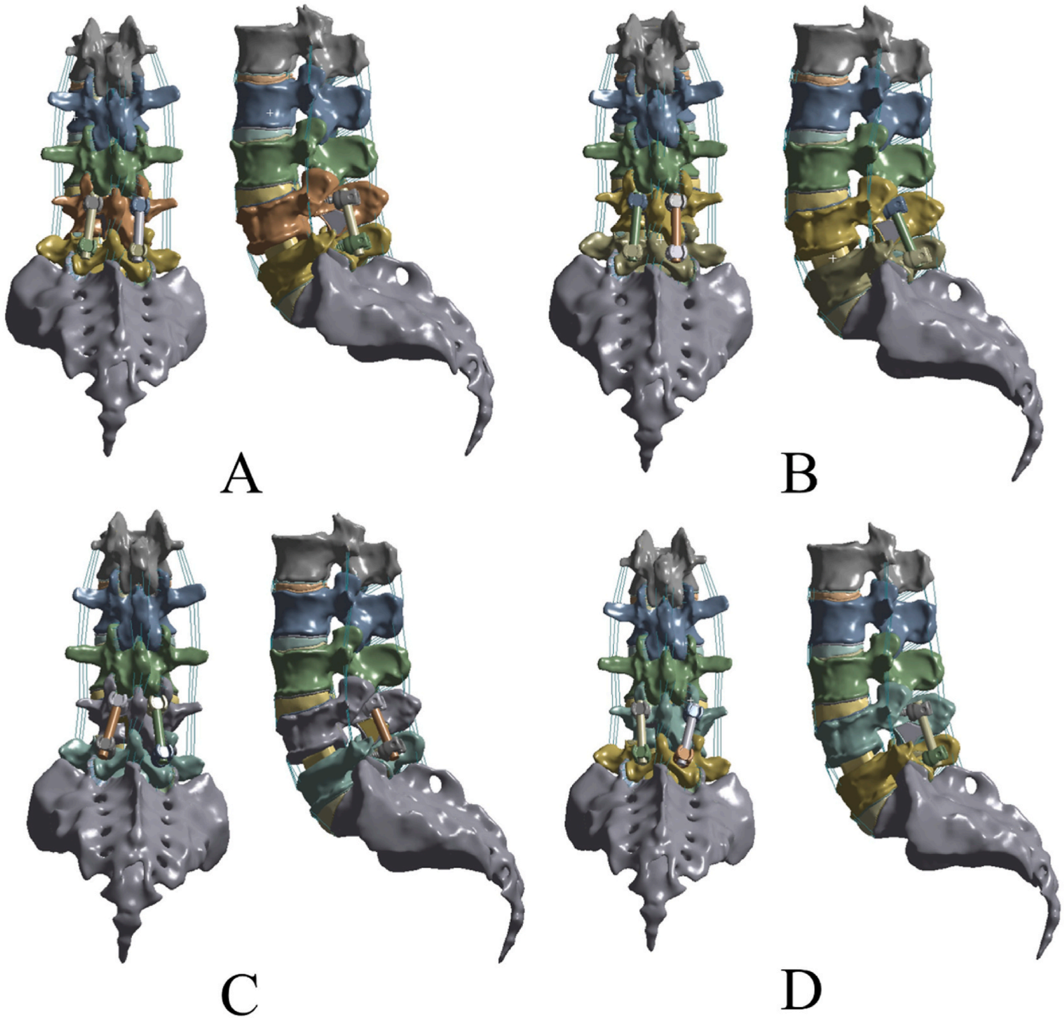


**Fig. 2.** Finite Element models of the L1-S1 lumbar spine with TLIF at the L4-L5 segment with four different fixation techniques. A: BCS-BCS; B: BMCS-BMCS; C: BMCS-BCS; D: BCS-BMCS.

endplate, enabling the application of loads and torques during the finite element analysis. The interaction between the vertebral bodies and intervertebral discs (cage) uses the tie restrictions. A 400 N compressive load is always vertically exerted on the central reference point of the endplate of the L1 vertebral body throughout the whole analysis. At the same time, the torque of 7.5 Nm is also applied on this point through three distinct anatomical planes: the X–Y plane representing the horizontal plane, the Y-Z plane representing the sagittal plane, and the X-Z plane representing the coronal plane to replicate four working conditions namely flexion, extension, bending, and rotation (Fig. 3 [17]). Specifically, a load of 7.5 Nm is applied along the Y positive (extension) and negative (flexion) axes of the model through the reference point to simulate the vertebral body undergoing flexion and extension. Similarly, to simulate lateral bending and rotation of the vertebral body, a load of 7.5 Nm was applied in the X and Z axes, respectively.

### 2.3. Measured items

The range of motion (ROM) of the L4-L5 segment, as well as the von Mises stress of the screws, intervertebral cage, and rods are measured in order to assess the biomechanical characteristics of different fixation techniques.

### 2.4. Model validation

The validation of the intact finite element models includes two steps. First, perform a mesh convergence analysis on one of the three complete Finite Element (FE) models. For this particular finite element model, except the standard mesh element size of 0.3 mm, meshes with sizes of 0.2 mm and 0.4 mm were incorporated to conduct a mesh convergence analysis. According to Ayturk et al. [27], axial rotation is the motion most sensitive to the mesh resolution in FE models. Simulating rotational conditions under a torque of 7.5 Nm and comparing the von Mises stress of different components, the convergence of the grid is considered when the difference in predicted results obtained from two consecutive grid resolutions is less than 5% [27]. This study uses the same method to compare the differences in von Mises stresses among the three meshes. In the second step, a torque of 7.5 Nm and a compressive load of 400 N are applied at the top of the model to simulate flexion, extension, lateral bending, and rotation. The ROM of the intact model in each segment is compared with the existing finite element models in previous research.

### 2.5. Statistical analysis

SPSS 28.0 software (IBM, Armonk, NY, USA) is used for data analysis. The data are expressed as the mean ± standard deviation. Prior to conducting the one-way ANOVA test, the normality of the data pertaining to four fixation techniques across three finite element models is assessed. It is found that all datasets have a normal distribution. The analysis of differences in data regarding four fixation techniques in flexion, extension, lateral bending, and rotation working conditions is conducted using One-way ANOVA and Post hoc tests (when the variances are equal, LSD is chosen, otherwise chosen T2). A significance level of $P < 0.05$ is used to determine statistical significance.

## 3. Results

### 3.1. Model validation

First, during the analysis of mesh convergence, different mesh qualities are utilized. Mesh 1 is characterized by an element size of

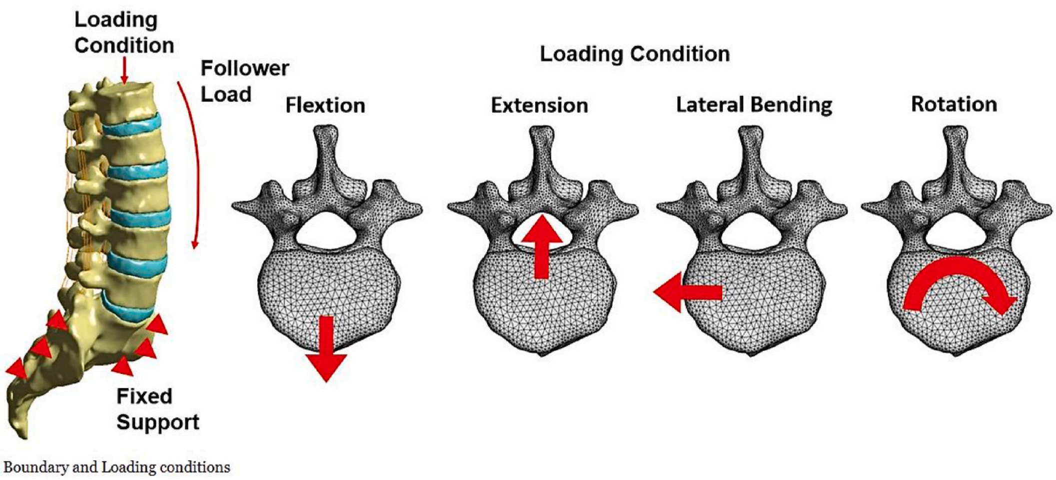


**Fig. 3.** Schematic diagram of torque loading [17].

0.4 mm, an average of 1,852,176 elements, and 2,122,491 nodes. Mesh 2 has an element size of 0.3 mm, an average of 2,114,420 elements, and 2,449,366 nodes. Lastly, Mesh 3 features an element size of 0.2 mm, an average of 2,497,843 elements, and 2,920,278 nodes. Among the three meshes, it is seen that Mesh 1 exhibits the lowest count of elements and nodes, whereas Mesh 3 demonstrates the largest count of elements and nodes. Fig. 4 depicts the percentage disparity in von Mises stress values between mesh 1 and mesh 3, as well as between mesh 2 and mesh 3. The cortical bone exhibits the highest disparity in projected von Mises stress between mesh 1 and mesh 3, with a magnitude of 4.06%. The slightest discrepancy in von Mises stress is observed between mesh 2 and 3 when considering all model components. Hence, mesh 2 demonstrates stress convergence (Fig. 4).

Second, the ROM in the entire model for each segment exhibited a resemblance to the findings and patterns of variation seen in the investigations conducted by Yamamoto et al. and Huang et al. (Fig. 5). Furthermore, Fig. 5 demonstrates that the ROM at different segment variation trends is also consistent. The findings indicate that the L1-S1 Finite element models created in this research are robustly produced and may be effectively employed for biomechanical investigation.

### 3.2. ROM of the L4-L5 segment

The ROMs for the L4-5 lumbar segment under flexion condition of BCS-BCS, BMCS-BMCS, BMCS-BCS, BCS-BMCS techniques are $0.53 \pm 0.16^\circ$, $0.53 \pm 0.16^\circ$, $0.68 \pm 0.08^\circ$, and $0.63 \pm 0.08^\circ$, respectively, with no statistical difference between groups ($F = 1.064$, $p = 0.417$). Under extension condition, the ROMs are $0.54 \pm 0.06^\circ$, $0.55 \pm 0.09^\circ$, $0.58 \pm 0.02^\circ$, and $0.53 \pm 0.05^\circ$, respectively, also with no statistical difference between the groups ($F = 0.373$, $p = 0.775$). However, under lateral bending conditions, the ROMs are $0.78 \pm 0.10^\circ$, $0.46 \pm 0.05^\circ$, $0.39 \pm 0.04^\circ$, and $0.49 \pm 0.04^\circ$, respectively, and a statistically significant difference is found between the groups ($F = 22.55$, $p < 0.001$). Meanwhile, under the rotation condition, the ROMs are $0.82 \pm 0.14^\circ$, $0.45 \pm 0.05^\circ$, $0.37 \pm 0.03^\circ$, and $0.49 \pm 0.04^\circ$, respectively, and the difference between the groups is also statistically significant ($F = 20.91$, $p < 0.001$), as shown in Fig. 6. For intergroup comparison with ROM under the same working condition by different fixation techniques, refer to Table 3.

### 3.3. Von mises stress of the intervertebral cage

The stresses on the intervertebral cage under flexion condition of the BCS-BCS, BMCS-BMCS, BMCS-BCS, BCS-BMCS techniques are $71.60 \pm 7.12$ MPa, $81.37 \pm 3.10$ MPa, $83.63 \pm 3.08$ MPa, and $57.90 \pm 12.01$ MPa, respectively, with a statistically significant difference between the groups ($F = 9.299$, $p = 0.006$). Under the extension condition, the stress values are $62.36 \pm 6.15$ MPa, $76.22 \pm 2.22$ MPa, $78.19 \pm 11.10$ MPa, and $50.70 \pm 16.50$ MPa, respectively, with a significant statistical difference observed between the groups ($F = 4.543$, $p = 0.039$). However, under lateral bending conditions, the stress values are $69.75 \pm 3.52$ MPa, $77.84 \pm 7.03$ MPa, $76.40 \pm 8.50$ MPa, and $64.71 \pm 3.27$ MPa, respectively, with no statistical difference between the groups ($F = 3.084$, $p = 0.090$). Under rotation condition, the stress values are $44.43 \pm 2.01$ MPa, $77.40 \pm 6.06$ MPa, $65.75 \pm 6.47$ MPa, and $60.58 \pm 2.26$ MPa, respectively, and a statistically significant difference is found between the groups ($F = 25.619$, $p < 0.001$), as shown in Fig. 7. For intergroup comparisons with cage stress under the same condition by different screw placement techniques, refer to Table 4.

### 3.4. Von mises stress of the screws

Under four different fixation techniques (BCS-BCS, BMCS-BMCS, BMCS-BCS, BCS-BMCS), the stresses on the screws under flexion conditions are $149.81 \pm 6.28$ MPa, $45.79 \pm 22.08$ MPa, $62.94 \pm 13.40$ MPa, and $108.67 \pm 8.31$ MPa, respectively, with a statistically

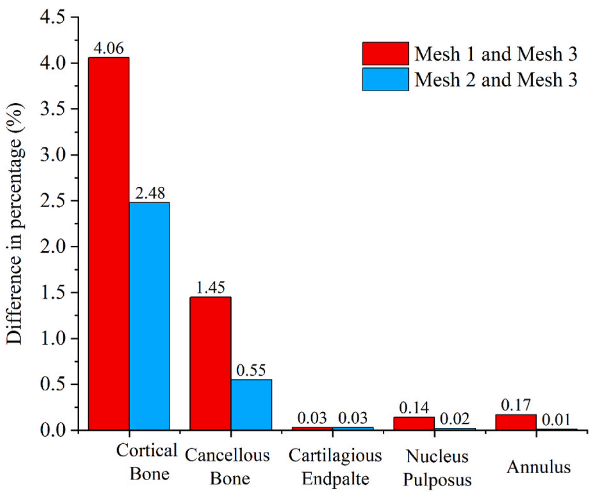


**Fig. 4.** Predicted percentage differences of the von Mises stress between Mesh 1 and Mesh 3 and between Mesh 2 and Mesh 3 for sample in the axial rotation [17].

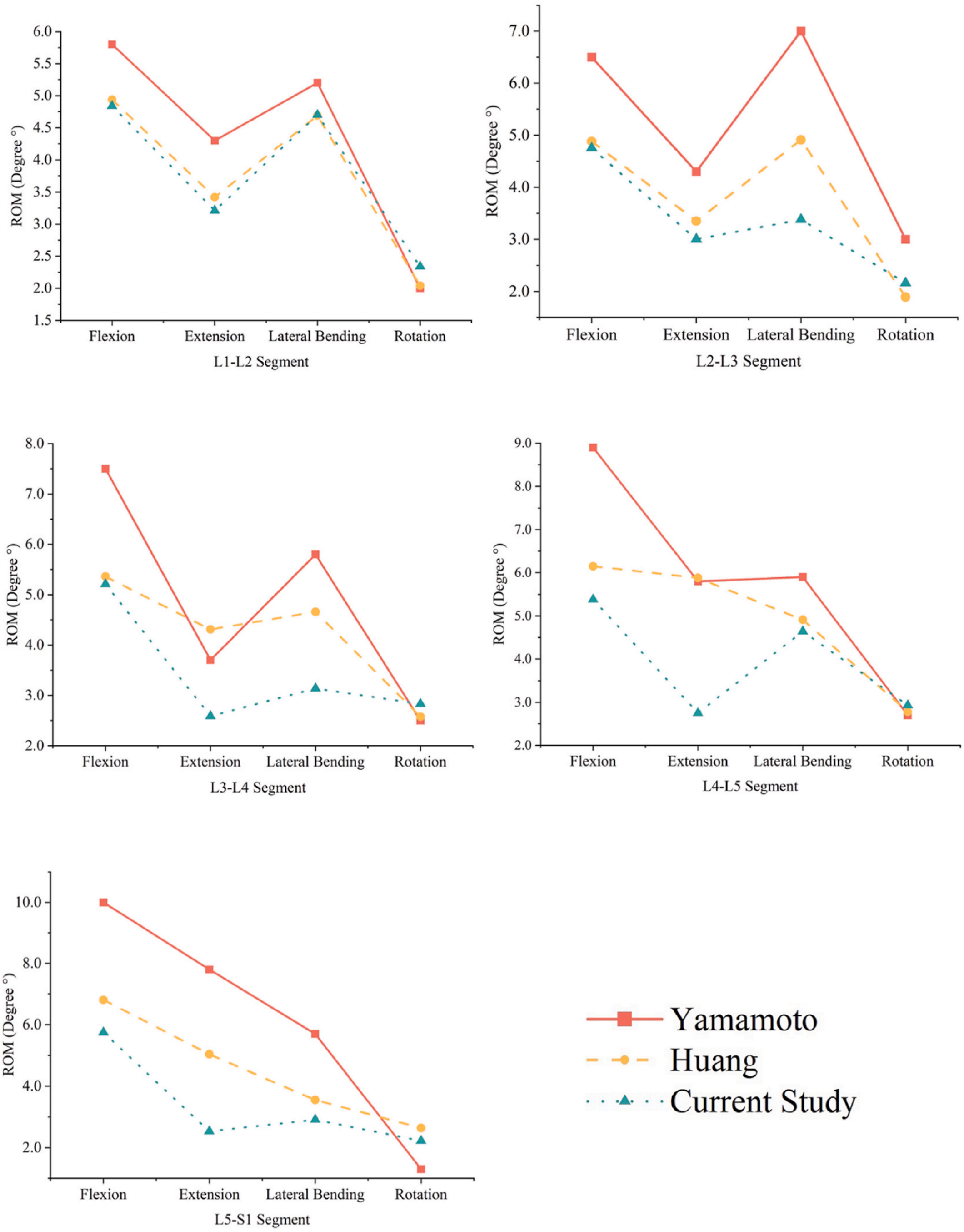


**Fig. 5.** Comparison of ROM of each segment between the current intact FE model and the previous studies.

significant difference observed between the groups (F = 34.262, p < 0.001). Under extension conditions, these values are 151.12 ± 6.70 MPa, 164.03 ± 8.63 MPa, 153.70 ± 17.97 MPa, and 162.61 ± 15.80 MPa, respectively, with no significant statistical difference between the groups (F = 0.713, p = 0.571). The stresses under lateral bending conditions are 247.51 ± 37.55 MPa, 107.80 ± 10.21 MPa, 130.42 ± 17.85 MPa, and 172.23 ± 5.90 MPa, respectively, with a significant statistical difference between the groups (F = 24.253, p < 0.001). Under rotation conditions, the stresses on the screws are 204.19 ± 10.17 MPa, 119.93 ± 13.62 MPa, 144.98 ± 28.86 MPa, and 175.81 ± 4.26 MPa, respectively, with a statistically significant difference found between the groups (F = 14.138, p = 0.001), as shown in Fig. 8. For intergroup comparisons with screw stresses under the same condition by different screw placement techniques, refer to Table 5. The distribution of screw stress under the four conditions with the four screw placement techniques is illustrated in Fig. 9.

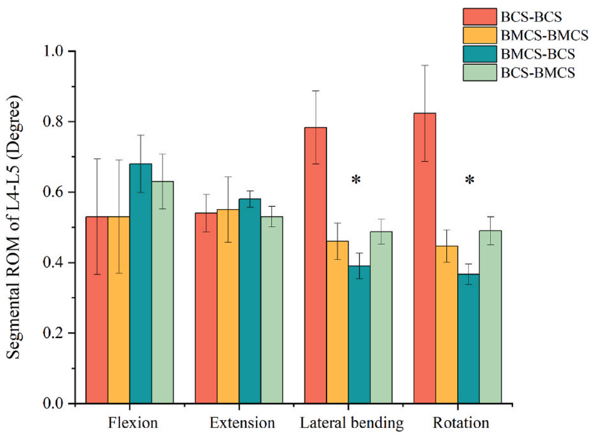


**Fig. 6.** ROM of L4-L5 segment
(* means there is a significant difference between fixation techniques).

**Table 3**
Comparison of ROM under the same working conditions with different fixation techniques.

| I (Hybrid screw trajectory mode) | | | BCS-BCS | | | BMCS-BMCS | | BMCS-BCS |
|---|---|---|---|---|---|---|---|---|
| J (Hybrid screw trajectory mode) | | | BMCS-BMCS | BMCS-BCS | BCS-BMCS | BMCS-BCS | BCS-BMCS | BCS-BMCS |
| Flexion (LSD) | I-J Mean Difference | | 0.000 | −0.153 | −0.100 | −0.153 | −0.100 | 0.053 |
| | Significance (p-value) | | 1.000 | 0.181 | 0.367 | 0.181 | 0.367 | 0.624 |
| | 95% CI | Lower Limit | −0.241 | −0.395 | −0.341 | −0.395 | −0.341 | −0.188 |
| | | Upper Limit | 0.241 | 0.088 | 0.141 | 0.088 | 0.141 | 0.295 |
| Extension (LSD) | I-J Mean Difference | | −0.007 | −0.037 | 0.013 | −0.030 | 0.020 | 0.050 |
| | Significance (p-value) | | 0.895 | 0.476 | 0.792 | 0.557 | 0.694 | 0.337 |
| | 95% CI | Lower Limit | −0.120 | −0.150 | −0.100 | −0.143 | −0.093 | −0.063 |
| | | Upper Limit | 0.106 | 0.076 | 0.126 | 0.083 | 0.133 | 0.163 |
| Lateral bending (LSD) | I-J Mean Difference | | 0.323 | 0.393 | 0.297 | 0.070 | −0.027 | −0.097 |
| | Significance (p-value) | | <0.001* | <0.001* | <0.001* | 0.213 | 0.620 | 0.099 |
| | 95% CI | Lower Limit | 0.204 | 0.274 | 0.177 | −0.049 | −0.146 | −0.216 |
| | | Upper Limit | 0.443 | 0.513 | 0.416 | 0.189 | 0.093 | 0.023 |
| Rotation (LSD) | I-J Mean Difference | | 0.377 | 0.457 | 0.333 | 0.080 | −0.043 | −0.123 |
| | Significance (p-value) | | <0.001* | <0.001* | 0.001* | 0.234 | 0.506 | 0.083 |
| | 95% CI | Lower Limit | 0.233 | 0.313 | 0.190 | −0.063 | −0.187 | −0.267 |
| | | Upper Limit | 0.520 | 0.600 | 0.477 | 0.223 | 0.100 | 0.020 |

* means significance.

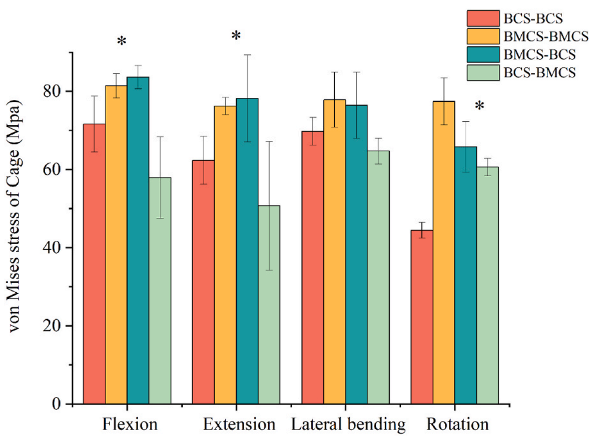


**Fig. 7.** Von Mises stress of the intervertebral cage at L4-L5 segment
(* means there is a significant difference between fixation techniques).

**Table 4**
Comparison of Max von Mises stress of cage under the same working conditions with different fixation techniques.

| I (Hybrid screw trajectory mode) | | | BCS-BCS | | | BMCS-BMCS | | BMCS-BCS |
|---|---|---|---|---|---|---|---|---|
| J (Hybrid screw trajectory mode) | | | BMCS-BMCS | BMCS-BCS | BCS-BMCS | BMCS-BCS | BCS-BMCS | BCS-BMCS |
| Flexion (LSD) | I-J Mean Difference | | −9.765 | −12.030 | 13.697 | −2.265 | 23.462 | 25.727 |
| | Significance (p-value) | | 0.110 | 0.058 | 0.036* | 0.688 | 0.003* | 0.001* |
| | 95% CI | Lower Limit | −22.286 | −24.552 | 1.176 | −14.787 | 10.940 | 13.206 |
| | | Upper Limit | 2.757 | 0.492 | 26.219 | 10.256 | 35.984 | 38.249 |
| Extension (LSD) | I-J Mean Difference | | −13.861 | −15.836 | 11.663 | −1.975 | 25.524 | 27.499 |
| | Significance (p-value) | | 0.250 | 0.523 | 0.923 | 1.000 | 0.513 | 0.409 |
| | 95% CI | Lower Limit | −42.567 | −59.380 | −64.367 | −63.872 | −71.812 | −33.872 |
| | | Upper Limit | 14.845 | 27.707 | 87.693 | 59.922 | 122.860 | 88.870 |
| Lateral bending (LSD) | I-J Mean Difference | | −13.861 | −15.836 | 11.663 | −1.975 | 25.524 | 27.499 |
| | Significance (p-value) | | 0.143 | 0.101 | 0.209 | 0.823 | 0.017* | 0.012* |
| | 95% CI | Lower Limit | −33.567 | −35.543 | −8.043 | −21.682 | 5.818 | 7.793 |
| | | Upper Limit | 5.845 | 3.870 | 31.369 | 17.731 | 45.230 | 47.206 |
| Rotation (LSD) | I-J Mean Difference | | −32.963 | −21.314 | −16.137 | 11.649 | 16.826 | 5.177 |
| | Significance (p-value) | | <0.001* | 0.001* | 0.003* | 0.016* | 0.002* | 0.213 |
| | 95% CI | Lower Limit | −41.779 | −30.130 | −24.953 | 2.833 | 8.009 | −3.640 |
| | | Upper Limit | −24.146 | −12.497 | −7.321 | 20.465 | 25.642 | 13.993 |

* means significance.

### 3.5. *Von mises stress of the rod*

Under four different fixation techniques (BCS-BCS, BMCS-BMCS, BMCS-BCS, BCS-BMCS), the stresses on the rod under flexion conditions are 39.64 ± 3.01 MPa, 32.88 ± 0.49 MPa, 33.78 ± 5.33 MPa, and 35.68 ± 2.75 MPa, respectively, with no statistically significant difference between the groups ($F = 2.836$, $p = 0.145$). In extension conditions, these values are 72.36 ± 7.71 MPa, 67.97 ± 2.00 MPa, 63.54 ± 0.81 MPa, and 69.17 ± 0.30 MPa, respectively, again showing no significant statistical difference between the groups ($F = 2.498$, $p = 0.134$). The stresses under lateral bending conditions are 103.06 ± 13.05 MPa, 74.78 ± 2.32 MPa, 78.11 ± 3.18 MPa, and 101.19 ± 13.88 MPa, respectively, with a statistically significant difference observed between the groups ($F = 7.047$, $p = 0.012$). Under rotational conditions, the stresses on the connecting rods are 90.85 ± 53.02 MPa, 47.61 ± 1.44 MPa, 53.80 ± 2.99 MPa, and 67.24 ± 9.58 MPa, respectively, with no significant statistical difference between the groups ($F = 1.512$, $p = 0.284$), as shown in Fig. 10. For intergroup comparisons with rod stresses under the same condition by different screw placement techniques, refer to Table 6. The distribution of rod stress under the four conditions with the four screw placement techniques is illustrated in Fig. 11.

It is noteworthy to notice that the four fixations consistently exhibit specific ordering across diverse conditions, encompassing flexion, extension, lateral bending, and rotation, in relation to the load applied to screws and rods. In particular, the BCS-BCS demonstrates the most elevated stress levels on both screws and rods, then succeeded by the BCS-BMCS, BMCS-BCS, and ultimately, the BMCS-BMCS. However, it is important to acknowledge that there is a notable discrepancy in the distribution of stress patterns between screws and rods across the four various working conditions for a particular internal fixation technique. For the connecting rods, it is seen that each method of fixation consistently demonstrates the maximum stress levels on the rods when exposed to lateral bending, followed by extension and rotation, while flexion results in the lowest stress on the rods. In the context of screws, diverse methods of fixation consistently demonstrate minimal stress on the screws in flexion. Nevertheless, the level of stress endured by screws during

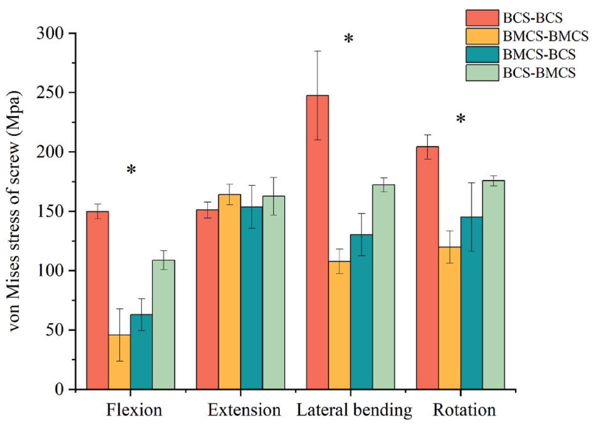


**Fig. 8.** Von Mises stress of the screws at L4-L5 segment
(* means there is a significant difference between fixation techniques).

**Table 5**
Comparison of Max von Mises stress of screw under the same working conditions with different fixation techniques.

| I (Hybrid screw trajectory mode) | | | BCS-BCS | | | BMCS-BMCS | | BMCS-BCS |
|---|---|---|---|---|---|---|---|---|
| J (Hybrid screw trajectory mode) | | | BMCS-BMCS | BMCS-BCS | BCS-BMCS | BMCS-BCS | BCS-BMCS | BCS-BMCS |
| Flexion (LSD) | I-J Mean Difference | | 104.025 | 86.864 | 41.143 | −17.160 | −62.881 | −45.721 |
| | Significance (p-value) | | <0.001* | <0.001* | <0.001* | 0.168 | 0.001* | <0.001* |
| | 95% CI | Lower Limit | 77.893 | 70.776 | 25.055 | −43.292 | −89.013 | −61.809 |
| | | Upper Limit | 130.156 | 102.953 | 57.232 | 8.971 | −36.750 | −29.633 |
| Extension (LSD) | I-J Mean Difference | | −12.907 | −2.577 | −11.487 | 10.330 | 1.420 | −8.910 |
| | Significance (p-value) | | 0.264 | 0.816 | 0.316 | 0.364 | 0.898 | 0.431 |
| | 95% CI | Lower Limit | −37.666 | −27.336 | −36.246 | −14.430 | −23.340 | −33.670 |
| | | Upper Limit | 11.853 | 22.183 | 13.273 | 35.090 | 26.180 | 15.850 |
| Lateral bending (LSD) | I-J Mean Difference | | 139.702 | 117.083 | 75.280 | −22.619 | −64.423 | −41.803 |
| | Significance (p-value) | | <0.001* | <0.001* | 0.003* | 0.236 | 0.006* | 0.041* |
| | 95% CI | Lower Limit | 99.015 | 76.396 | 34.593 | −63.307 | −105.110 | −82.491 |
| | | Upper Limit | 180.390 | 157.771 | 115.967 | 18.068 | −34.593 | −1.116 |
| Rotation (LSD) | I-J Mean Difference | | 84.260 | 59.215 | 28.380 | −25.045 | −55.880 | −30.835 |
| | Significance (p-value) | | <0.001* | 0.003* | 0.073 | 0.107 | 0.004* | 0.056 |
| | 95% CI | Lower Limit | 52.480 | 27.434 | −3.401 | −56.826 | −87.661 | −62.615 |
| | | Upper Limit | 116.041 | 90.995 | 60.161 | 6.735 | −24.100 | 0.946 |

* means significance.

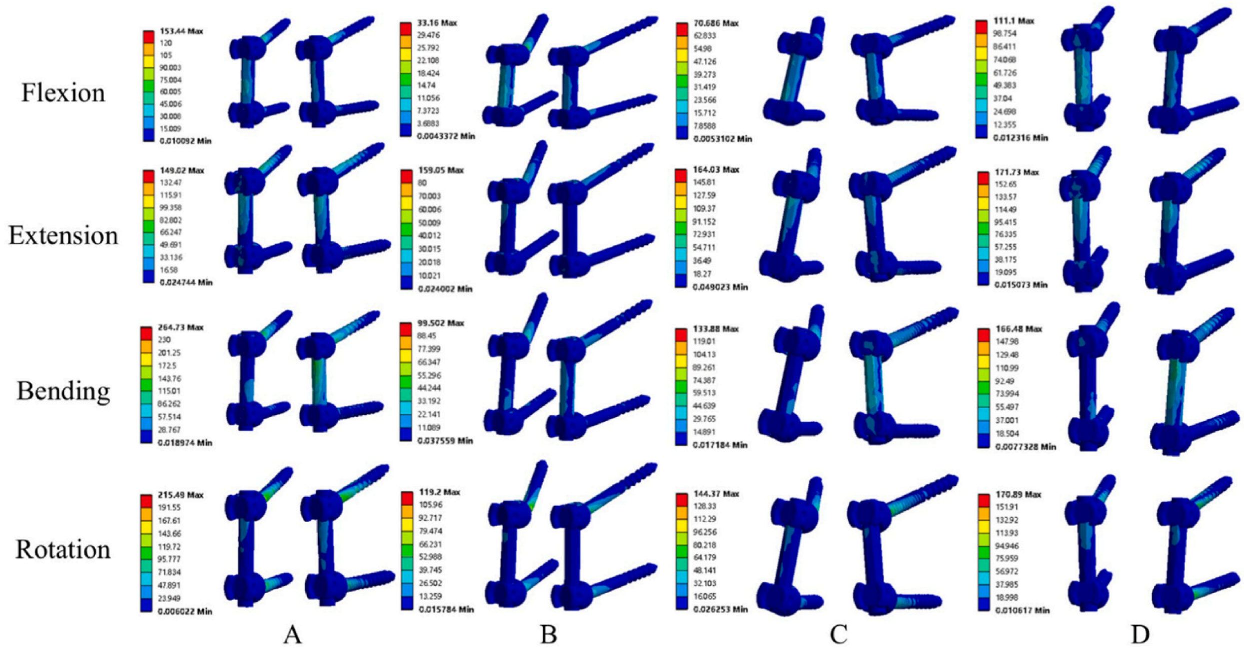


**Fig. 9.** Stress nephograms over the screws of four different fixation techniques (BCS-BCS, BMCS-BMCS, BMCS-BCS, BCS-BMCS) in flexion, extension, bending, and rotation working conditions. A: the BCS-BCS group. B: the BMCS-BMCS group. C: the BMCS-BCS group, and D: the BCS-BMCS group.

extension, lateral bending, and rotation is dependent on the specific fixation technique employed and does not exhibit a clear and consistent pattern similar to that observed with rods. For details, see Fig. 12.

## 4. Discussion

The TLIF procedure was initially documented in 1982 and was originally employed for treating spondylolisthesis. It has now become one of the most common procedures for lumbar interbody fusion, which limits the disturbance to the canal, alleviates excessive traction on nerve roots and the dural sac, and mitigates the likelihood of cerebrospinal fluid leakage and nerve injury [28]. Furthermore, the TLIF technique is advantageous in conserving the non-operative side of the vertebral lamina and facet joint, hence contributing to the preservation of spinal stability in contrast to the PLIF procedure [8]. Nevertheless, the TLIF approach does have certain limitations, including the occurrence of muscle atrophy at the surgical site and potential harm to the facet joints on the

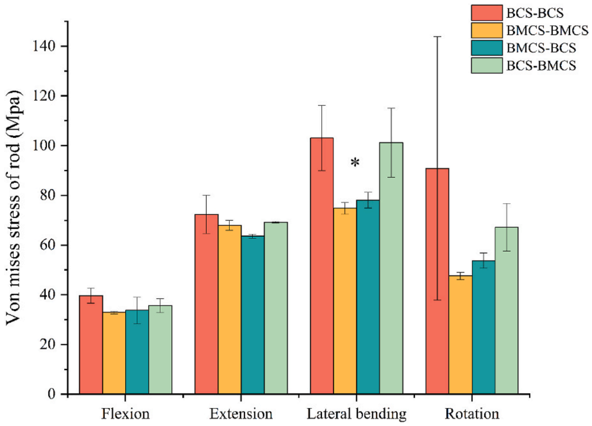


**Fig. 10.** Von Mises stress of the rods at L4-L5 segment
(* means there is a significant difference between fixation techniques).

**Table 6**
Comparison of Max von Mises stress of rod under the same working conditions with different fixation techniques.

| I (Hybrid screw trajectory mode) | | | BCS-BCS | | | BMCS-BMCS | | BMCS-BCS |
|---|---|---|---|---|---|---|---|---|
| J (Hybrid screw trajectory mode) | | | BMCS-BMCS | BMCS-BCS | BCS-BMCS | BMCS-BCS | BCS-BMCS | BCS-BMCS |
| Flexion (LSD) | I-J Mean Difference | | 6.760 | 5.852 | 3.959 | −0.908 | −2.801 | −1.893 |
| | Significance (p-value) | | 0.039* | 0.066 | 0.187 | 0.749 | 0.337 | 0.510 |
| | 95% CI | Lower Limit | 0.430 | −0.478 | −2.371 | −7.237 | −9.130 | −8.222 |
| | | Upper Limit | 13.089 | 12.181 | 10.288 | 5.421 | 3.528 | 4.436 |
| Extension (LSD) | I-J Mean Difference | | 4.391 | 8.823 | 3.187 | 4.432 | −1.204 | −5.636 |
| | Significance (p-value) | | 0.966 | 0.706 | 0.991 | 0.249 | 0.956 | 0.018* |
| | 95% CI | Lower Limit | −35.954 | −37.572 | −44.503 | −4.495 | −12.869 | −9.352 |
| | | Upper Limit | 44.736 | 55.218 | 50.877 | 13.359 | 10.461 | −1.920 |
| Lateral bending (LSD) | I-J Mean Difference | | 28.282 | 24.952 | 1.880 | −3.330 | −26.402 | −23.072 |
| | Significance (p-value) | | 0.007* | 0.014* | 0.819 | 0.686 | 0.01* | 0.02* |
| | 95% CI | Lower Limit | 9.969 | 6.638 | −16.434 | −21.644 | −44.716 | −41.385 |
| | | Upper Limit | 46.595 | 43.265 | 20.193 | 14.983 | −8.089 | −4.759 |
| Rotation (LSD) | I-J Mean Difference | | 43.241 | 37.057 | 23.612 | −6.184 | −19.629 | −13.444 |
| | Significance (p-value) | | 0.085 | 0.131 | 0.315 | 0.271 | 0.345 | 0.553 |
| | 95% CI | Lower Limit | −7.579 | −13.763 | −27.208 | −18.572 | −75.493 | −60.718 |
| | | Upper Limit | 94.061 | 87.877 | 74.432 | 6.203 | 36.235 | 33.829 |

* means significance.

operational side [29]. The lumbar muscles are of significant importance in maintaining spinal stability, as evidenced by earlier studies that have established a strong correlation between the loosening of the S1 pedicle screw and the degenerative changes occurring in the adjacent musculature [30]. The posterior midline approach is frequently employed in TLIF surgery, wherein the deep fascia is incised along the spinous process, and the paraspinal muscles are dissected to provide visualization of the lamina and facet joints [31]. The screw entry point of the CBT and MCBT shift interior, compared to PS, enables the insertion of MCBT or CBT screws through the TLIF fusion surgical incision, resulting in reduced muscle damage and alignment with the principles of minimally invasive surgery, as advocated in contemporary surgical practice [32].

This study did not find statistically significant variations in the ROMs at the L4-5 segment when comparing the four different fixation procedures under both flexion and extension working conditions. Nevertheless, the spine's stability differed across four fixation procedures when subjected to lateral bending and rotation. In general, the BMCS-BCS technique exhibited the greatest degree of spinal stability, with the BMCS-BMCS technique ranking second, followed by BCS-BMCS, and ultimately BCS-BCS.

Prior research has indicated that the performance of CBT technology is suboptimal when subjected to lateral bending and rotating working conditions, which may be attributed to the comparatively shorter length of the CBT screw and hindered its ability to adequately stabilize the anterior column of the spine [33]. Hence, the BCS-BCS fixation technique has the lowest level of stability. On the other hand, the MCBT technique, which is rooted in the CBT technique, has demonstrated enhancements in cephalic angle reduction, lateral angle increase, and screw length increase, which helps to serve to further augment the contact area between the screw and the cortical bone of the pedicle as well as the upper endplate. In the study conducted by McLachlin et al., it was observed that loose screws frequently exhibit a phenomenon referred to as the "teeter-totter", wherein the tail end of the screw remains stationary while the head end is capable of movement [34]. In contrast to CBT, MCBT offers the advantage of securing both the head and tail ends of a screw within the cortical bone. Specifically, the head end is fixed in the cortical bone of the upper endplate, while the tail end is

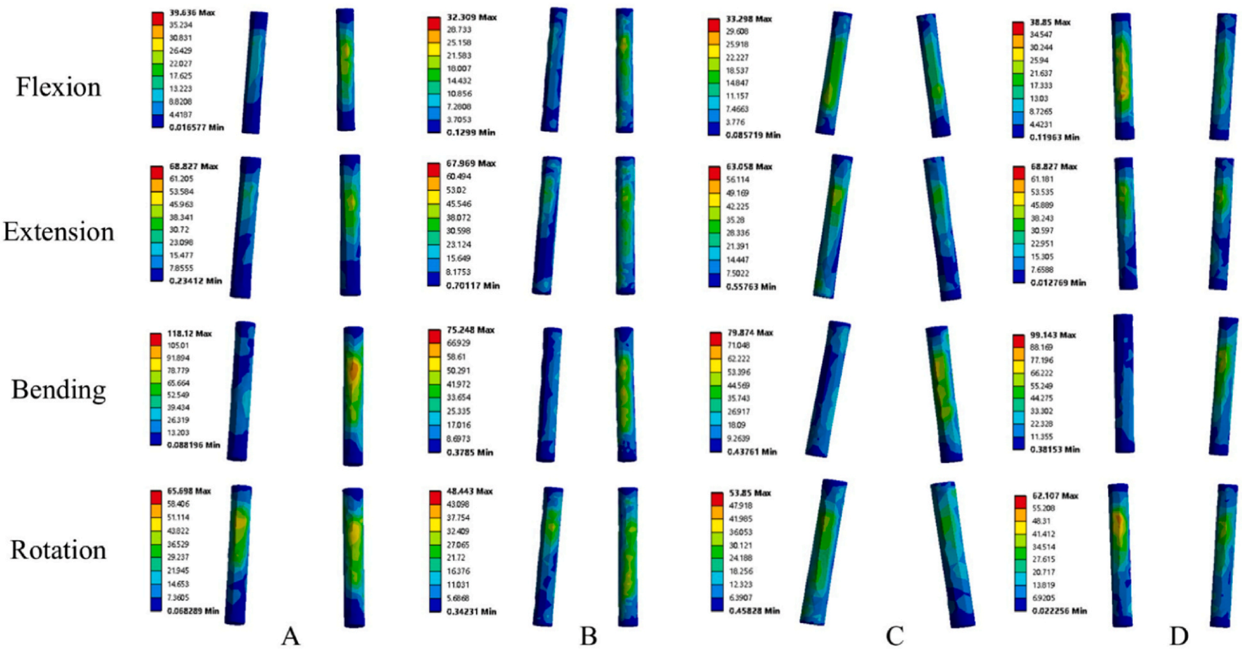


**Fig. 11.** Stress nephograms over the rods of four different fixation techniques (BCS-BCS, BMCS-BMCS, BMCS-BCS, BCS-BMCS) in flexion, extension, bending, and rotation working conditions. A: the BCS-BCS group. B: the BMCS-BMCS group. C: the BMCS-BCS group, and D: the BCS-BMCS group.

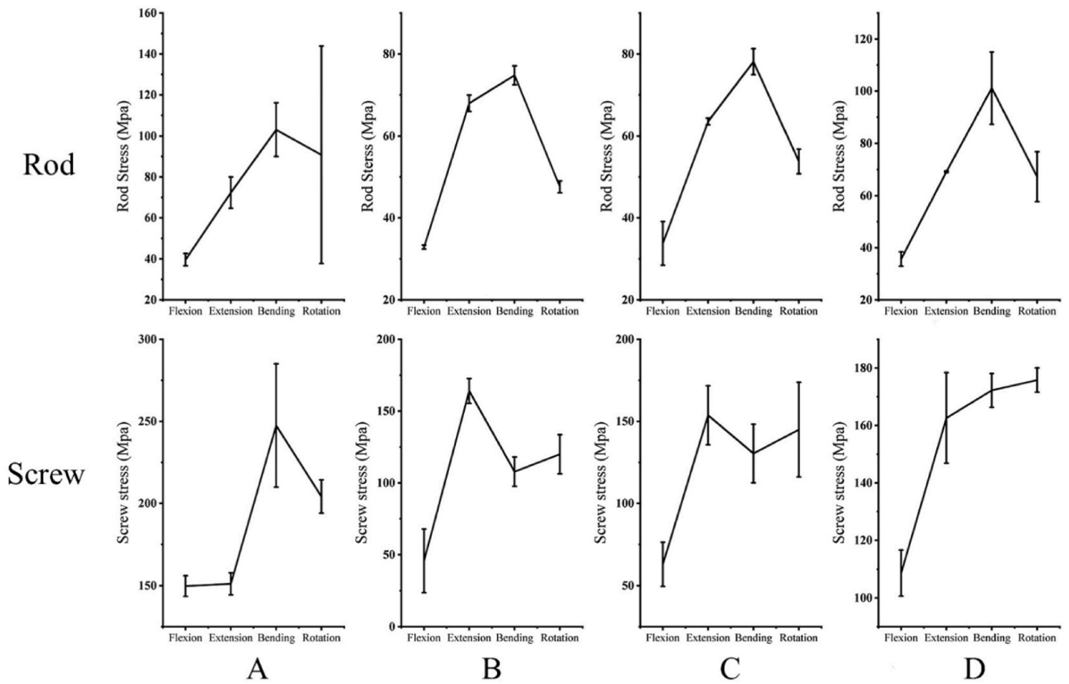


**Fig. 12.** The variations in the stress of screws and rods of four different fixation techniques (BCS-BCS, BMCS-BMCS, BMCS-BCS, BCS-BMCS) in flexion, extension, bending, and rotation working conditions
A: the BCS-BCS group. B: the BMCS-BMCS group. C: the BMCS-BCS group, and D: the BCS-BMCS group.

fixed in the cortical bone of the pedicle. So, the MCBT technique effectively reduces the occurrence of the "teeter-totter" phenomenon and enhances the screw's resistance to lateral bending and rotation. The L4 vertebra demonstrates more mobility compared to L5 in spinal movement, leading to elevated stress on the screw located at the L4 level, which means the ROM of the L4-5 segment is mostly influenced by the technique employed for placing the L4 screw [35]. Under conditions of flexion and extension, both CBT and MCBT exhibit comparable biomechanical characteristics, while when subjected to lateral bending and axial rotation circumstances, the MCBT exhibits enhanced biomechanical performance compared to the CBT. So, the discrepancy in ROM between the fixation technique utilizing MCBT technology at L4 segments and the fixation technique employing CBT technology at L4 segments can be attributed to the above-mentioned factors.

In comparison to ROM, the cage within the BMCS-BCS technology experiences the highest levels of stress when subjected to flexion, extension, and lateral bending, subsequently followed by the BMCS-BMCS, BCS-BCS, and BCS-BMCS technologies, in sequential order. In contrast, under rotational conditions, the cage in the BMCS-BMCS technology demonstrates the highest level of stress, followed by the BMCS-BCS, BCS-BMCS, and BCS-BCS technologies. In terms of stress distribution, it can be observed that screws and rods, which are internal fixation systems, in four fixation techniques, exhibit a more stable order throughout all four working conditions, with the order of BCS-BCS > BCS-BMCS > BMCS-BCS > BMCS-BMCS.

Previous research has demonstrated a positive correlation between the maximum stress experienced by the cage and the rate at which the cage settles [36]. At present, there exists a lack of agreement among experts regarding the optimal kind of fixation for mitigating cage settlement. Nevertheless, it is widely acknowledged among researchers that the utilization of a hybrid fixation technique has the potential to enhance the stability of the surgical segment and mitigate the occurrence of cage settling [37]. This perspective aligns with the findings of the present study, wherein the BMCS-BCS technique demonstrated superior postoperative spinal stability (Low ROM), while the BCS-BMCS technique exhibited the lowest peak stress on the fusion device. Moreover, the research findings of Pei, Zhang, Su, and other scholars have also demonstrated the minimum peak stress experienced by screws and connecting rods when subjected to flexion or extension conditions, which aligns with the outcomes obtained in the present study [37–39]. It is hypothesized that this phenomenon could potentially be associated with the increased mechanical strain experienced by the vertebral body's osseous tissue during flexion or extension movements.

Based on the preceding narration, the stress magnitude sequence in screws and rods within four fixation techniques remains consistent across four distinct working conditions. However, the manner in which the stress of screw and rod in different fixation methods alter varies under working conditions. Overall, of the four fixation techniques, the rod experiences its highest stress level during lateral bending compared to the other three working conditions, whereas the maximum stress of the screws is distributed among four different working conditions. This phenomenon occurs probably due to the rod primarily receiving the stress transmitted by the screws, which originates from a single source and is less affected by other tissues. Under the lateral bending condition, the stress becomes localized on a single rod, leading to an unequal distribution and an increase in the magnitude of the peak stress. However, the fluctuation of stress in screws is more intricate. The screws serve the dual ways of stress flow, which means they not only transmit stress to both the cage and rod but also potentially experience extra stress from the fusion device and connecting rod. Therefore, the maximum stress in screws is dispersed across four working conditions.

The stress distribution diagram derived from the finite element analysis offers valuable insights into the interaction and influence of stress inside the intervertebral cage, screws, and rod. However, there is a dearth of scholarly research that investigates the association between these three components of stress, so one of the primary objectives of this work is to provide a comprehensive understanding of the interplay between stress factors. The stress diagram reveals that the internal fixation system undergoes notable stress concentration, principally on the upper screw and rod, during flexion, extension, and lateral bending conditions. Under axial rotation conditions, the stress encountered by the lower screw increases, greater than cage stress, although at a lesser degree compared to the upper screw and rod. The alteration of the maximum stress experienced by the cage within different fixation techniques can be related to the transfer of stress from the fusion device to the screw through the surrounding tissues, reducing the stress on the cage itself, while the screw will likewise convey stress to the fusion device indirectly through the surrounding tissues. The direction of stress transfer mainly depends on the relative stress size between the two components, that is, the transfer from the component with higher stress to the component with lower stress. Generally, within the working condition of flexion, extension, and lateral bending, the sequence of stress among the superior screw, cage, and inferior screw follows a relationship where the highest stress is observed in the superior screw, followed by the cage, and finally, the inferior screw, which suggests that there is a transfer of stress from the upper screw to the fusion cage, and then from the fusion cage to the lower screw. But under rotational working conditions, the stress of the lower screw is more considerable than the cage, which means both upper and lower screws would transmit stress to the cage. In addition to the previously mentioned mechanism of indirect stress transmission, it is essential to acknowledge that the superior screw possesses the ability to directly transfer stress to the inferior screw through the utilization of a connecting rod. According to the idea of the shielding effect, stress propagation primarily happens in materials with similar elastic moduli, which implies that stress transmission primarily takes place within the internal fixation system [37]. Therefore, it is imperative to prioritize the direct transmission pathway over the aforementioned indirect transmission pathway, which is crucial for achieving a well-balanced stress distribution in the internal fixation system. However, in this study, all four fixation approaches have a direct transmission channel. As a result, the primary influence on the stress distribution inside the internal fixation system is exerted mainly by the indirect transmission pathway. Consequently, our upcoming research will be dedicated to examining the process of indirect stress transmission.

In the context of flexion, extension, and lateral bending working conditions, the upper screw of the BCS-BMCS technique is relatively short, leading to a longer distance between the screw head end and the cage, which means the superior screw exhibits a diminished capacity to efficiently transmit stress in an indirect pathway to the cage, while the cage has the potential to transmit the load to the longer, inferior MCBT screw indirectly, hence leading to limited peak stress on the fusion cage. This also means that the internal fixation system within the BCS-BMCS technique has to endure additional stress from the cage to exhibit tremendous internal fixation system stress in theory. However, in reality, the stress distribution per unit length of the overall internal fixation system is relatively minimal due to the long inferior MCBT screw, which leads to the actual internal fixation stress being smaller than that of the BCS-BCS technique. In contrast, the BMCS-BCS technique is characterized by a longer upper MCBT screw, enabling efficient stress transmission to the cage, while the inferior CBT screws, being shorter in length, exhibit limited capacity to effectively receive stress from the fusion cage. In this scenario, it is imperative for the fusion cage to not only endure its inherent stress but also accommodate the extra stress imposed by the internal fixation system. Consequently, the fusion device within the BMCS-BCS technique experiences the highest peak stress among the four fixation procedures. Simultaneously, as a result of stress transmission from screws to the cage, the maximum stress experienced by the internal fixation system in the context of the BMCS-BCS technique is comparatively lower than that observed in the BCS-BCS and BCS-BMCS techniques, however remains higher than the stress encountered in the BMCS-BMCS technique. It is posited that the phenomenon is because the BMCS-BMCS technique has more complete stress transfer pathways, as compared to alternative fixation procedures, which means that in addition to the direct transmission of stress, this technique also involves a complete indirect stress transfer pathway for screw stress allows stress originating from the upper screws to be indirectly transmitted to the lower screws via the fusion device. Hence, compared to alternative methods of screw placement, the internal fixation system in BMCS-BMCS methodology exhibits a more evenly distributed stress distribution. Moreover, within the context of the BMCS-BMCS technique, it is worth noting that both the upper and lower screws possess the longest lengths in four fixation techniques that lead to a reduced stress distribution per unit length, hence minimizing the peak stress in the internal fixation system. Not likely to the stress experienced in the internal fixation system within the BMCS-BMCS technique, the peak stress of the cage is higher in the BMCS-BMCS technique than in the BCS-BCS and BCS-BMCS techniques. This phenomenon can be attributed to the disparity in the length of the upper screw within the BMCS-BMCS technique compared to the BCS-BCS and BCS-BMCS techniques. Specifically speaking, the elongated length of the upper screw in the BMCS-BMCS technique facilitates a more seamless transmission of stress to the fusion device, while in the BCS-BCS technique, the upper screw is unable to transfer stress to the fusion device effectively, and the fusion device is also unable to transfer stress to the lower screw so the internal fixation system exhibits a relatively low influence on the stress levels experienced by the fusion device, with cage's peak stress ranking second only to that of the BCS-BMCS technique. Also, due to the reduced length of the upper and lower screws in the BCS-BCS technique, there is an increased stress distribution per unit length, exhibiting the highest peak stress in the internal fixation system. In contrast to flexion, extension, and lateral bending conditions, the stress experienced by the lower screw surpasses that of the fusion cage during rotational conditions, which leads the stress flow direction to change, resulting in the transfer of stress from the lower screw to the fusion device. Therefore, the BMCS-BMCS technique has the highest intervertebral cage stress and the lowest internal fixation stress, while the BCS-BCS technique has the lowest intervertebral cage stress and the highest internal fixation stress.

After comprehensively analyzing the results of finite element analysis, it can be concluded that among the four fixed techniques, the BMCS-BCS technique and BMCS-BMCS technique have superior comprehensive mechanical performance. Both the BMCS-BCS and BMCS-BMCS techniques exhibit a comparatively low ROM and internal fixation stress, hence contributing to the preservation of postoperative spinal stability and a decrease in the likelihood of breakage and loss of internal fixation devices. However, among these two techniques with similar mechanical performance, our inclination is to recommend the BMCS-BCS hybrid fixation technique.

Currently, endoscopic fusion technology is continuously developed [40]. As a minimally invasive screw technique, CBT technology allows for the placement of screws close to the decompression area of the lumbar spine, which means the placement of screws can be done under endoscopic guidance, followed by subsequent decompression and fusion surgery. As opposed to the CBT technique, MCBT technology involves inward screw entry points, which is relatively far from the decompression area of the lumbar spine, so performing endoscopic decompression during the implantation of MCBT screws may lead to potentially poorer decompression effects. According to a study conducted by Pank and Kleinstueck [41,42], utilizing larger fusion cages can effectively transfer fusion stress uniformly over the vertebral endplate, leading to enhanced stability of the lumbar surgical segment. In contrast to CBT screws, MCBT screws have a position that is in close proximity to the central spinal canal. The utilization of MCBT technology in the fixation technique's lower screw may present challenges for the implantation of larger fusion cages, potentially limiting the options to just small or expandable fusion cages, so in such scenarios, CBT technology emerges as a more favorable choice. Additionally, when employing the identical screw technique for both the upper and lower screws, the direction of stress transmission is relatively single, leading to an uneven distribution of stress load between the upper and lower vertebrae [43]. In contrast, the utilization of distinct screw techniques for the upper and lower vertebrae leads to varying stress transmission directions in the upper and lower screws during spinal movement, resulting in a more homogeneous distribution of stress in the superior and inferior vertebrae, thereby enhancing the stability of the operative segment. This is also why the ROM in the BMCS-BCS is smaller than in the BMCS-BMCS.

In the preceding paragraph, the reasons that contribute to the superiority of BMCS-BCS technology over BMCS-BMCS technology with regard to decompression fusion and spinal stability when performed under endoscopy are examined. Next, in this paragraph, a more in-depth analysis will be conducted to assess the benefits of BMCS-BCS technology within the realm of clinical practice. The existing body of literature indicates that following spinal fusion procedures, there is a high prevalence of degeneration in the segment immediately adjacent to the fused site, especially the first segment above the fused segments, known as Adjacent Segment Degeneration (ASD) [44,45]. The phenomenon can be attributed to the relocation of the spinal motion center towards the proximal segment following spinal fusion and fixation, leading to an augmented compensatory of the neighboring segment, which is recognized as a significant factor of patient prognosis [46,47]. Furthermore, it is well acknowledged among researchers that the occurrence of ASD can also be attributed to the detrimental effects (such as damage) on the intervertebral disc and facet joints during surgery [48]. From an anatomical standpoint, the BMCS-BCS technique has efficacy in reducing the ASD incidence of the first segment located proximal to the fusion site, thereby leading to an enhancement in the patient's overall prognosis. The cause lies in the fact that the upper side MCBT screws have a larger lateral angle and a smaller cephalic angle compared to CBT, and even in the event of an inadvertent screw penetrating the vertebral body during surgical procedures, the site of penetration typically occurs around the upper endplate border of the lumbar vertebral body where only involves the outer part of the intervertebral disc fibrous ring. So, the MCBT screws mitigate the risk of ASD by avoiding the issue of intervertebral disc damage caused by the pointed tip of CBT screws protruding at the upper endplate position corresponding to the nucleus pulposus. Moreover, it is noteworthy that the screw entry point of the MCBT is notably situated in an inward manner, with the screw tail positioned at a considerable distance from the facet joint, so the likelihood of any potential collision between the screw tail and the facet joint during spinal movement is diminished, thereby minimizing the probability of sustaining a facet joint injury. On the other hand, the tip of the lower side CBT screw in the context of the BMCS-BCS technique can provide support underneath the upper endplate corresponding to the surgical segment's cage, which helps alleviate the settling of the fusion cage under greater peak stress. Prior research has indicated that increased stress on the fusion device can result in inadequate intervertebral height and the loss of physiological curvature, in turn leading to the development of fixation segmental kyphosis, which may subsequently cause lower limb pain, difficulties with walking, and potentially even nerve damage [49]. While the BMCS-BCS fusion cage exhibits slightly greater peak stress, the observed increase is not statistically significant compared to the other three fixation techniques. However, this technique has significant advantages in terms of the ROM and stress level of the internal fixation system compared to other fixation techniques. Therefore, the higher peak stress of the fusion cage in this technique is acceptable.

While it is true that the BMCS-BMCS technique has certain drawbacks as compared to the BMCS-BCS technique in relation to endoscopic decompression fusion, vertebral stability, and patient prognosis, it is nevertheless advisable to employ the BMCS-BMCS fixation technique for individuals who have severe osteoporosis. The reason for this is that CBT techniques have been found to have limited effectiveness in patients with severe osteoporosis; in concrete terms, CBT techniques still tend to loosen in patients with severe osteoporosis. In contrast, MCBT techniques increase the contact area between the screw and the thicker inner and inferior cortical bone of the vertebral pedicle through a larger lateral angle, smaller cephalic angle, and inward entry point, thereby increasing the CT value around the trajectory, making it more suitable for patients with severe osteoporosis [50]. Even though BMCS-BMCS technology exhibits a greater fusion peak stress in four fixation techniques, it is essential to note that in cases involving patients with severe osteoporosis, the primary objective of fusion internal fixation surgery should be to augment the stability of the internal fixation system. In this context, BMCS-BMCS exhibits the lowest levels of internal fixation stress and a reduced ROM, catering to the requirements of fusion internal fixation procedures in individuals with severe osteoporosis.

This research examines the biomechanical properties of hybrid CBT and MCBT fixation techniques within an intact lumbar-sacral finite element model, marking a novel contribution to this field. Nevertheless, it is imperative to acknowledge the existence of some constraints. Firstly, there exists a prevailing academic opinion that the musculature connected to the spinal column has a beneficial stabilizing influence on the movement of the spine [51,52]. It has been reported that patients undergoing CBT screw fixation have a lower postoperative blood creatine kinase concentration than those using pedicle screw, suggesting a reduced extent of muscle tissue damage in CBT screw fixation [48]. However, the model in this research has not rebuilt muscle tissue, potentially leading to suboptimal biomechanical performance with the CBT and MCBT techniques. Secondly, the analysis conducted in the study did not encompass an examination of the effects of the hybrid fixation techniques within the TLIF approach on the adjacent segments. Hence, the current stress distribution in the adjacent disc of the TLIF model under the hybrid fixation technique remains uncertain, posing challenges in accurately forecasting the occurrence rate of ASD. Thirdly, this study did not discuss the differences in the effects of using screws with different diameters and lengths, which could potentially impact the biomechanical performance of the internal fixation system. Finally, it should be noted that the study's sample size is small, consisting of only three specimens, which implies that the results may be subject to the constraints imposed by the sample size, and additional validation and exploration ought to be carried out using a more extensive sample size in further study. Although there have been some advancements in the mechanical performance of hybrid fixation techniques in this study, it is essential to re-phrase that the conclusion conducted thus far is based on preliminary findings and has not yet concluded conclusive results due to the small sample size. In order to obtain more reliable and comprehensive conclusions, it is necessary to overcome the limitations mentioned above in future finite element analysis and cadaver and animal testing studies to get a relatively deciding conclusion.

## 5. Conclusion

The objective of this study is to explore the biomechanical properties of four distinct hybrid fixation techniques when utilized in conjunction with the TLIF technique, using a finite element model of the complete lumbosacral spine. Among the four hybrid fixation techniques, the BMCS-BCS technique exhibited supremacy biomechanical performance, characterized by low ROM and the peak stress of the internal fixation system, as well as acceptable peak stress in the fusion cage. The mechanical performance of the BMCS-BMCS technique is comparable to that of the BMCS-BCS technique. However, the BMCS-BMCS technique exhibited a greater contact area between the screw and the cortical bone of the vertebrae, rendering it a more appropriate choice for patients afflicted with severe osteoporosis. Albeit the BCS-BMCS and BCS-BCS techniques exhibited lower peak stress within the cage, they demonstrated hefty ROM and the peak stress of the internal fixation system, which may lead to potential instability in the operative segment and failure of the internal fixation system, making them unsuitable for patients with severe degeneration of the spine.

## Funding

This study is supported by the Xinjiang Uyghur Autonomous Region Natural Science Fund for Distinguished Young Scholars (Grant No. 2021D01E29), Major Project of Science and Technology Program of Xinjiang Uygur Autonomous Region (Grant No. 2022A03011).

## Ethics approval and consent to participate

The study design was approved by the Ethics Committee of Xinjiang Medical University before data collection and analysis

(Approval No.20210401–01). All methods are carried out in accordance with relevant guidelines and regulations.

## Consent for publication

All procedures were conducted in accordance with the ethical standards of the Declaration of Helsinki. The three cadaveric specimens used in the study were obtained from individuals who had signed body donation agreements. This agreement explicitly stated their voluntary consent for the use of their bodies in medical education and scientific research. Based on these agreements, the Ethics Committee waived the informed consent. The study design was approved by the Ethics Committee of First Affiliated Hospital of Xinjiang Medical University before data collection and analysis (Approval No. 20210401–01). All methods were carried out in accordance with relevant guidelines and regulations.

## Data availability statement

The raw data supporting the conclusion of this article will be made available on request.

## CRediT authorship contribution statement

**Yixi Wang:** Writing – review & editing, Writing – original draft, Visualization, Validation, Methodology, Data curation, Conceptualization. **Abulikemu Maimaiti:** Writing – review & editing, Software, Methodology, Formal analysis, Conceptualization. **Yang Xiao:** Writing – review & editing, Resources, Conceptualization. **Abudusalamu Tuoheti:** Software, Formal analysis. **Rui Zhang:** Software, Formal analysis. **Muzaipaer Maitusong:** Software. **Qihao Chen:** Resources, Data curation. **Paerhati Rexiti:** Writing – review & editing, Writing – original draft, Visualization, Project administration, Methodology, Funding acquisition, Formal analysis, Data curation, Conceptualization.

## Declaration of competing interest

The authors declare that they have no known competing financial interests or personal relationships that could have appeared to influence the work reported in this paper.

## Acknowledgments

We thank Ruo-Xuan Fu (The University of Utah, USA), Yu-Qiao Tang (Northeastern University, USA), Alafate Kahaer (Tsinghua University, China), Lin-Huan Lei (Southwest University, China) for their contributions to improving and evaluating the language of the article. We also thank Yi-Shan Ding (Columbia University, USA) for her help with statistics.

## References

[1] B.G. Santoni, R.A. Hynes, K.C. McGilvray, G. Rodriguez-Canessa, A.S. Lyons, M.A.W. Henson, W.J. Womack, C.M. Puttlitz, Cortical bone trajectory for lumbar pedicle screws, Spine J. 9 (2009) 366–373, https://doi.org/10.1016/j.spinee.2008.07.008.

[2] S. Guo, K. Zhu, M.-J. Yan, X.-H. Li, J. Tan, Cortical bone trajectory screws in the treatment of lumbar degenerative disc disease in patients with osteoporosis, World J Clin Cases 10 (2022) 13179–13188, https://doi.org/10.12998/wjcc.v10.i36.13179.

[3] A.A. Momin, M.P. Steinmetz, Evolution of minimally invasive lumbar spine surgery, World Neurosurg 140 (2020) 622–626, https://doi.org/10.1016/j.wneu.2020.05.071.

[4] H.A. Fenton-White, Trailblazing: the historical development of the posterior lumbar interbody fusion (PLIF), Spine J. 21 (2021) 1528–1541, https://doi.org/10.1016/j.spinee.2021.03.016.

[5] R.J. Mobbs, K. Phan, G. Malham, K. Seex, P.J. Rao, Lumbar interbody fusion: techniques, indications and comparison of interbody fusion options including PLIF, TLIF, MI-TLIF, OLIF/ATP, LLIF and ALIF, J Spine Surg 1 (2015) 2–18, https://doi.org/10.3978/j.issn.2414-469X.2015.10.05.

[6] R. Verma, S. Virk, S. Qureshi, Interbody fusions in the lumbar spine: a review, HSS J. 16 (2020) 162–167, https://doi.org/10.1007/s11420-019-09737-4.

[7] M.C. Prabhu, K.C. Jacob, M.R. Patel, H. Pawlowski, N.N. Vanjani, K. Singh, History and Evolution of the minimally invasive transforaminal lumbar interbody fusion, Neurospine 19 (2022) 479–491, https://doi.org/10.14245/ns.2244122.061.

[8] S.L. de Kunder, S.M.J. van Kuijk, K. Rijkers, I.J.M.H. Caelers, W.L.W. van Hemert, R.A. de Bie, H. van Santbrink, Transforaminal lumbar interbody fusion (TLIF) versus posterior lumbar interbody fusion (PLIF) in lumbar spondylolisthesis: a systematic review and meta-analysis, Spine J. 17 (2017) 1712–1721, https://doi.org/10.1016/j.spinee.2017.06.018.

[9] I. Teng, J. Han, K. Phan, R. Mobbs, A meta-analysis comparing ALIF, PLIF, TLIF and LLIF, J. Clin. Neurosci. 44 (2017) 11–17, https://doi.org/10.1016/j.jocn.2017.06.013.

[10] J.-W. Kwon, Y. Park, B.H. Lee, S.Y. Park, C.K. Lim, J.H. Yang, J.-W. Ha, K.-S. Suk, S.-H. Moon, H.-S. Kim, A comparison between cortical bone trajectory screws and traditional pedicle screws in patients with single-level lumbar degenerative spondylolisthesis: five-year results, Spine 48 (2023) 1617–1625, https://doi.org/10.1097/BRS.0000000000004523.

[11] P. Rexiti, D. Aikeremu, S. Wang, N. Abuduwali, A. Kahaer, W. Sheng, Cadaveric study of anatomical measurement of isthmus parameters of lumbar spine to guide cortical bone screw placement, Rev. Assoc. Med. Bras. 68 (2022) 754–758, https://doi.org/10.1590/1806-9282.20210729.

[12] P. Rexiti, T. Abudurexiti, N. Abuduwali, S. Wang, W. Sheng, Measurement of lumbar isthmus parameters for novel starting points for cortical bone trajectory screws using computed radiography, Am J Transl Res 10 (2018) 2413–2423.

[13] P. Rexiti, G. Aierken, S. Wang, T. Abudurexiti, N. Abuduwali, Q. Deng, H. Guo, W. Sheng, Anatomical research on strength of screw track fixation in novel cortical bone trajectory for osteoporosis lumbar spine, Am J Transl Res 11 (2019) 6850–6859.

[14] Y.-X. Wang, J. Maitirouzi, S.-Q. Wang, R. Zhang, X. Zeng, W. Nuerhazi, H.-T. Yang, Z.-H. Zhou, P. Rexiti, Finite element analysis on biomechanical properties of traditional trajectory and modified cortical bone trajectory, J. Med. Biomechanics 37 (2022) 485–491, https://doi.org/10.16156/j.1004-7220.2022.03.016.

[15] Z.-H. Zhou, J. Maitirouzi, S.-Q. Wang, A. Kahaer, P. Rexiti, Comparison of biomechanical properties between traditional and modified cortical bone trajectory technique, Journal of Xinjiang Medical University 45 (2022) 1129–1133, https://doi.org/10.3969/j.issn.1009-5551.2022.10.009.

[16] Z.-H. Zhou, A. Kahaer, Y.-X. Wang, D.-S. Liu, X. Maimaiti, W.-J. Shi, P. Rexiti, Biomechanical properties of traditional trajectory screw technique and modified cortical bone trajectory technique: a finite element analysis, Chinese Journal of Tissue Engineering Research 26 (2022) 2789–2794, https://doi.org/10.12307/2022.682.

[17] A. Kahaer, R. Zhang, Y. Wang, H. Luan, A. Maimaiti, D. Liu, W. Shi, T. Zhang, H. Guo, P. Rexiti, Hybrid pedicle screw and modified cortical bone trajectory technique in transforaminal lumbar interbody fusion at L4-L5 segment: finite element analysis, BMC Muscoskel. Disord. 24 (2023) 288, https://doi.org/10.1186/s12891-023-06385-y.

[18] A. Kahaer, X. Maimaiti, J. Maitirouzi, S. Wang, W. Shi, N. Abuduwaili, Z. Zhou, D. Liu, A. Maimaiti, P. Rexiti, Biomechanical investigation of the hybrid modified cortical bone screw–pedicle screw fixation technique: finite-element analysis, Front Surg 9 (2022), https://doi.org/10.3389/fsurg.2022.911742.

[19] T. Zander, A. Rohlmann, G. Bergmann, Influence of different artificial disc kinematics on spine biomechanics, Clin. BioMech. 24 (2009) 135–142, https://doi.org/10.1016/j.clinbiomech.2008.11.008.

[20] H. Xu, W. Ju, N. Xu, X. Zhang, X. Zhu, L. Zhu, X. Qian, F. Wen, W. Wu, F. Jiang, Biomechanical comparison of transforaminal lumbar interbody fusion with 1 or 2 cages by finite-element analysis, Operative Neurosurgery 73 (2013) ons198, https://doi.org/10.1227/01.neu.0000430320.39870.f7. –ons205.

[21] K. Wang Md, C. Jiang PhD, L. Wang PhD, H. Wang Md, W. Niu PhD, The biomechanical influence of anterior vertebral body osteophytes on the lumbar spine: a finite element study, Spine J. 18 (2018) 2288–2296, https://doi.org/10.1016/j.spinee.2018.07.001.

[22] T. Zander, A. Rohlmann, G. Bergmann, Influence of different artificial disc kinematics on spine biomechanics, Clin. BioMech. 24 (2009) 135–142, https://doi.org/10.1016/j.clinbiomech.2008.11.008.

[23] H.-J. Kim, H.-J. Chun, H.-M. Lee, K.-T. Kang, C.-K. Lee, B.-S. Chang, J.S. Yeom, The biomechanical influence of the facet joint orientation and the facet tropism in the lumbar spine, Spine J. 13 (2013) 1301–1308, https://doi.org/10.1016/j.spinee.2013.06.025.

[24] R.N. Natarajan, K. Watanabe, K. Hasegawa, Biomechanical analysis of a long-segment fusion in a lumbar spine—a finite element model study, J. Biomech. Eng. 140 (2018), https://doi.org/10.1115/1.4039989.

[25] Y.M. Lu, W.C. Hutton, V.M. Gharpuray, Do bending, Twisting, and Diurnal fluid changes in the disc Affect the Propensity to Prolapse? A Viscoelastic finite element model, Spine 21 (1996) 2570–2579, https://doi.org/10.1097/00007632-199611150-00006.

[26] A. Kiapour, D. Ambati, R.W. Hoy, V.K. Goel, Effect of graded facetectomy on biomechanics of dynesys dynamic stabilization system, Spine 37 (2012), https://doi.org/10.1097/BRS.0b013e3182463775. E581–E589.

[27] U.M. Ayturk, C.M. Puttlitz, Parametric convergence sensitivity and validation of a finite element model of the human lumbar spine, Comput. Methods Biomech. Biomed. Eng. 14 (2011) 695–705, https://doi.org/10.1080/10255842.2010.493517.

[28] C.P. DiPaola, R.W. Molinari, Posterior lumbar interbody fusion, J. Am. Acad. Orthop. Surg. 16 (2008) 130–139, https://doi.org/10.5435/00124635-200803000-00004.

[29] P. Poppenborg, U. Liljenqvist, G. Gosheger, A. Schulze Boevingloh, L. Lampe, S. Schmeil, T.L. Schulte, T. Lange, Complications in TLIF spondylodesis-do they influence the outcome for patients? A prospective two-center study, Eur. Spine J. 30 (2021) 1320–1328, https://doi.org/10.1007/s00586-020-06689-w.

[30] J.-B. Kim, S.-W. Park, Y.-S. Lee, T.-K. Nam, Y.-S. Park, Y.-B. Kim, The effects of spinopelvic parameters and paraspinal muscle degeneration on S1 screw loosening, J Korean Neurosurg Soc 58 (2015) 357, https://doi.org/10.3340/jkns.2015.58.4.357.

[31] D.H. Ge, N.D. Stekas, C.G. Varlotta, C.R. Fischer, A. Petrizzo, T.S. Protopsaltis, P.G. Passias, T.J. Errico, A.J. Buckland, Comparative analysis of two transforaminal lumbar interbody fusion techniques, Spine (2019) 44, https://doi.org/10.1097/BRS.0000000000002903. E555–E560.

[32] S. Sharif, A. Afsar, Learning curve and minimally invasive spine surgery, World Neurosurg 119 (2018) 472–478, https://doi.org/10.1016/j.wneu.2018.06.094.

[33] L. Perez-Orribo, S. Kalb, P.M. Reyes, S.W. Chang, N.R. Crawford, Biomechanics of lumbar cortical screw-rod fixation versus pedicle screw-rod fixation with and without interbody support, Spine 38 (2013) 635–641, https://doi.org/10.1097/BRS.0b013e318279a95e.

[34] S.D. McLachlin, B.J.B. Beaton, M.T. Sabo, K.R. Gurr, S.I. Bailey, C.S. Bailey, C.E. Dunning, Comparing the fixation of a novel hollow screw versus a conventional solid screw in human sacra under cyclic loading, Spine 33 (2008) 1870–1875, https://doi.org/10.1097/BRS.0b013e3181808c75.

[35] M. Wu, S. Wang, S.J. Driscoll, T.D. Cha, K.B. Wood, G. Li, Dynamic motion characteristics of the lower lumbar spine: implication to lumbar pathology and surgical treatment, Eur. Spine J. 23 (2014) 2350–2358, https://doi.org/10.1007/s00586-014-3316-9.

[36] C. Nan, Z. Ma, Y. Liu, L. Ma, J. Li, W. Zhang, Impact of cage position on biomechanical performance of stand-alone lateral lumbar interbody fusion: a finite element analysis, BMC Muscoskel. Disord. 23 (2022) 920, https://doi.org/10.1186/s12891-022-05873-x.

[37] K.-C. Su, K.-H. Chen, C.-C. Pan, C.-H. Lee, Biomechanical evaluation of cortical bone trajectory fixation with traditional pedicle screw in the lumbar spine: a finite element study, Appl. Sci. 11 (2021) 10583, https://doi.org/10.3390/app112210583.

[38] L. Zhang, H.-M. Li, R. Zhang, H. Zhang, C.-L. Shen, Biomechanical changes of adjacent and fixed segments through cortical bone trajectory screw fixation versus traditional trajectory screw fixation in the lumbar spine: a finite element analysis, World Neurosurg 151 (2021) e447–e456, https://doi.org/10.1016/j.wneu.2021.04.061.

[39] B. Pei, Y. Xu, Y. Zhao, X. Wu, D. Lu, H. Wang, S. Wu, Biomechanical comparative analysis of conventional pedicle screws and cortical bone trajectory fixation in the lumbar spine: an in vitro and finite element study, Front. Bioeng. Biotechnol. 11 (2023), https://doi.org/10.3389/fbioe.2023.1060059.

[40] Y. Ahn, Endoscopic spine discectomy: indications and outcomes, Int. Orthop. 43 (2019) 909–916, https://doi.org/10.1007/s00264-018-04283-w.

[41] K. Phan, R.J. Mobbs, Evolution of design of interbody cages for anterior lumbar interbody fusion, Orthop. Surg. 8 (2016) 270–277, https://doi.org/10.1111/os.12259.

[42] F.S. Kleinstueck, S.S. Hu, D.S. Bradford, Use of allograft femoral rings for spinal deformity in adults, Clin. Orthop. Relat. Res. 394 (2002) 84–91, https://doi.org/10.1097/00003086-200201000-00010.

[43] B. Pei, Y. Xu, Y. Zhao, X. Wu, D. Lu, H. Wang, S. Wu, Biomechanical comparative analysis of conventional pedicle screws and cortical bone trajectory fixation in the lumbar spine: an in vitro and finite element study, Front. Bioeng. Biotechnol. 11 (2023), https://doi.org/10.3389/fbioe.2023.1060059.

[44] K. Hashimoto, T. Aizawa, H. Kanno, E. Itoi, Adjacent segment degeneration after fusion spinal surgery-a systematic review, Int. Orthop. 43 (2019) 987–993, https://doi.org/10.1007/s00264-018-4241-z.

[45] M.D. Helgeson, A.J. Bevevino, A.S. Hilibrand, Update on the evidence for adjacent segment degeneration and disease, Spine J. 13 (2013) 342–351, https://doi.org/10.1016/j.spinee.2012.12.009.

[46] C.K. Lee, Accelerated degeneration of the segment adjacent to a lumbar fusion, Spine 13 (1988) 375–377, https://doi.org/10.1097/00007632-198803000-00029.

[47] Y. Shono, K. Kaneda, K. Abumi, P.C. McAfee, B.W. Cunningham, Stability of posterior spinal instrumentation and its effects on adjacent motion segments in the lumbosacral spine, Spine 23 (1998) 1550–1558, https://doi.org/10.1097/00007632-199807150-00009.

[48] Y. Wang, A. Kahaer, A. Maimaiti, H. Guo, P. Rexiti, Complication, fusion, and revision rate in the lumbar cortical bone trajectory and pedicle screw fixation techniques: a systematic review and meta-analysis, J. Orthop. Surg. Res. 18 (2023) 382, https://doi.org/10.1186/s13018-023-03820-7.

[49] K. Satake, T. Kanemura, H. Nakashima, H. Yamaguchi, N. Segi, J. Ouchida, Cage subsidence in lateral interbody fusion with transpsoas approach: intraoperative endplate injury or late-onset settling, Spine Surg Relat Res 1 (2017) 203–210, https://doi.org/10.22603/ssrr.1.2017-0004.

[50] D. Liu, A. Kahaer, Y. Wang, R. Zhang, A. Maiaiti, X. Maimaiti, Z. Zhou, W. Shi, Z. Cui, T. Zhang, L. Li, P. Rexiti, Comparison of CT values in traditional trajectory, traditional cortical bone trajectory, and modified cortical bone trajectory, BMC Surg. 22 (2022) 441, https://doi.org/10.1186/s12893-022-01893-5.

[51] D. Kernc, V. Strojnik, R. Vengust, Early initiation of a strength training based rehabilitation after lumbar spine fusion improves core muscle strength: a randomized controlled trial, J. Orthop. Surg. Res. 13 (2018) 151, https://doi.org/10.1186/s13018-018-0853-7.

[52] D.L. Belavý, G. Armbrecht, C.A. Richardson, D. Felsenberg, J.A. Hides, Muscle atrophy and changes in spinal morphology: is the lumbar spine vulnerable after prolonged bed-rest? Spine 36 (2011) 137–145, https://doi.org/10.1097/BRS.0b013e3181cc93e8.